International Journal of Coal Geology 87 (2011) 97–111

Contents lists available at ScienceDirect

International Journal of Coal Geology

journal homepage: www.elsevier.com/locate/ijcoalgeo

Chemometric analysis of functional groups in fossil remains of the *Dicroidium* flora (Cacheuta, Mendoza, Argentina): Implications for kerogen formation

José A. D'Angelo [a,b,*], Leticia B. Escudero [c], Wolfgang Volkheimer [a], Erwin L. Zodrow [d]

[a] Instituto Argentino de Nivología, Glaciología y Ciencias Ambientales (IANIGLA)-CCT-CONICET-Mendoza, Avda. Ruiz Leal s/n Parque Gral. San Martín (5500) Mendoza, Argentina
[b] Área de Química, Instituto de Ciencias Básicas, Universidad Nacional de Cuyo, Centro Universitario, M5502JMA, Mendoza, Argentina
[c] Grupo de Investigación y Desarrollo en Química Analítica (QUIANID), (LISAMEN-CCT-CONICET-Mendoza) Mendoza, Argentina
[d] Palaeobotanical Laboratory, Cape Breton University, Sydney, Nova Scotia, Canada B1P 6L2

ARTICLE INFO

Article history:
Received 4 April 2011
Received in revised form 17 May 2011
Accepted 17 May 2011
Available online 23 May 2011

Keywords:
FTIR
Chemometric study
Gondwana Triassic
Argentina
Kerogen

ABSTRACT

Studied samples include eight Gondwanan species of the *Dicroidium* flora: seed ferns (3), conifer (1), cycad-related (1), unknown affinity gymnosperms (2), and one undetermined axis from two Middle to Upper Triassic localities (Cacheuta, Mendoza, central western Argentina). Based on differing preservation states and sample treatments, four sample forms are established: (1) compressions, (2) cuticles, (3) cuticle-free coalified layers, and (4) associated coal samples. The purpose of the study is firstly to analyze the sample forms using Fourier transform infrared (FTIR) spectrometry, contributing to filling an existing gap of chemical information for Gondwanan pant fossil remains. Secondly, semi-quantitative chemical parameters, calculated by area integration of infrared spectra, are treated using principal component analysis to infer statistical groupings as a function of chemical structures (functional groups). From the initial two-component solution, based on the 8×41 data matrix, a subset matrix (4×29) could be isolated which also yielded a two-component solution (in each case, cumulative explained variance is at least 89%). Results include the distinction between the coaly forms (1) compressions and (3) cuticle-free coalified layers mainly based on the carbonyl contents and branching and length of the hydrocarbon side chains. The highly aliphatic nature of cuticles, which is indicative of biomacromolecules (cutin), is noted. Similarities in functional groups are recorded with types of kerogen and coal macerals. The result enables us to postulate that the functional groups characterizing the different modes of preservation of our fossil remains are likely related to the propensity to generate oil and gas/condensate from the kerogen. Our data have the potential for future studies with implications for chemotaxonomy, molecular taphonomy, and paleoclimatology.

1. Introduction

The preservation of fossils in sediments depends mainly on the nature of the organism (e.g., invertebrate or plant cuticles), and the environment in which they are deposited (terrestrial or marine, euxinic or oxygenated). Nevertheless, diagenetic alteration to an aliphatic composition (the so-called diagenetic polymerization) exerts the biggest influence in the long-term preservation of the organic chemistry of animal and plant fossils (Briggs, 1999). During the last decades the processes involved in diagenetic transformations of sedimentary organic remains have started to be unraveled. The most decay-resistant molecules have been found in algae and vascular plants (e.g., Collinson et al., 1994, 1998; Largeau et al., 1990; Mösle et al., 1998; Nip et al., 1986a,b; Tegelaar et al., 1991; van Bergen et al., 2004; Zodrow et al., 2009, 2010; Zodrow and Mastalerz, 2001, 2002, 2007 and references therein).

Chemical knowledge of fossil remains preserving organic matter has greatly benefited from the development of advanced spectroscopic instrumentation. This is the case of Fourier transform infrared (FTIR) spectrometry which permits the direct analysis of samples without previous modifications (e.g., extraction, heating, etc.). A number of investigations have focused on the FTIR study of several plant groups from the Carboniferous of the Northern Hemisphere (e.g., D'Angelo et al., 2010; Lyons et al., 1995; Pšenička et al., 2005; Zodrow et al., 2000, 2003, 2009, 2010; Zodrow and Mastalerz, 2001, 2002, 2007).

Despite the wide occurrence of the *Dicroidium* flora throughout Gondwana, very little is known of its paleobiochemistry, or preserving organic matter of coalified remains (e.g., D'Angelo, 2006; Paull et al., 1998). Our initial FTIR studies of this fossil flora showed encouraging results. They proved to be useful for studies of lacustrine environments (D'Angelo and Volkheimer, 2007),

* Corresponding author at: Instituto Argentino de Nivología, Glaciología y Ciencias Ambientales (IANIGLA)-CCT-CONICET-Mendoza, Avda. Ruiz Leal s/n Parque Gral. San Martín (5500) Mendoza, Argentina. Fax: +54 261 5244201.
E-mail addresses: joseadangelo@yahoo.com (J.A. D'Angelo), lescudero@mendoza-conicet.gob.ar (L.B. Escudero), volkheim@lab.cricyt.edu.ar (W. Volkheimer), Erwin_Zodrow@cbu.ca (E.L. Zodrow).

0166-5162/$ – see front matter © 2011 Elsevier B.V. All rights reserved.
doi:10.1016/j.coal.2011.05.005

paleoclimatic parameters (Escudero et al., 2008), and some aspects of fossil preservation (D'Angelo et al., 2007; Zodrow et al., 2009).

The present study is based on a comparatively larger sample size including eight species not all of the same preservation type. We use the distribution and contents of functional groups derived from FTIR spectrometry to characterize the different sample forms. But more importantly, the chemical data lends itself to statistical analyses with potential to address questions of taphonomy and kerogen formation.

2. Stratigraphy of collection sites

Fossil remains from Triassic exposures were collected on the southern side of the Cacheuta Hill, Mendoza, western Argentina, from two previously undescribed stratigraphic Sections: 1) Puesto El Durazno and 2) Trinchera La Mary from the upper Potrerillos and the lower Cacheuta Formations, respectively (Fig. 1). These Triassic units are part of the Uspallata Group (Rolleri and Criado Roque, 1968; Stipanicic, 1979), which represents the most complete and best known continental Triassic succession of the Cuyana Basin (Stipanicic and Zavattieri, 2002). The latter is the largest continental Triassic rift basin of southern South America including several sub-basins (López Gamundí et al., 1994). The Triassic formations of the Uspallata Group comprise fluvial facies that range from alluvial fan to braided and meandering river, deltaic, and lacustrine facies (Jenchen and Rosenfeld, 2002). For details see Gallego (1992), Morel (1994), Marsicano et al. (2001), Zamuner et al. (2001), Morel and Povilauskas (2002), D'Angelo (2006) and Morel et al. (2010).

2.1. Puesto El Durazno locality

At Puesto El Durazno (33°04′43″ S, 69°07′11″ W, 1413 m above sea level, Fig. 1) the regional strike and dip are 120°/20° S. Outcrops include approximately 17 m of fine-grained clastic rocks (see Fig. 2) in which cuticle-free coalified layers (leaves without preserved cuticles, Table 1) are entombed. From the lowermost part upwards exposures are as follows:

(1) More than 70 cm of carbonaceous gray, brownish shale containing plant debris (upper part).
(2) 10 cm of medium-grained, sandy tuffite, with abundant muscovite.
(3) 55 cm of carbonaceous, gray brownish shale, intercalated with gray siltstone bearing plant debris.
(4) 8 cm of sandy medium-grained, tuffite, with abundant muscovite.
(5) 34 cm of carbonaceous, gray brownish plant-bearing shale.
(6) 12 cm of very hard, dark gray, tuffitic siltstone, bearing big carbonized plant remains and plant debris.
(7) 40 cm of carbonaceous, gray brownish shale, strongly weathered.
(8) 120 cm of alternating fine-grained, sandy tuffite and silty shale bearing abundant plant debris. The intervals of shale are partially covered.
(9) 4 m covered (not sampled).
(10) 500 cm alternation of carbonaceous, dark gray to black shale and intercalated brownish gray shale, with abundant coalified plant remains and some levels with secondary gypsum.
(11) 80 cm of alternating light brown shale and siltstone. In the upper third, cuticle-free coalified layers and non-marine bivalve

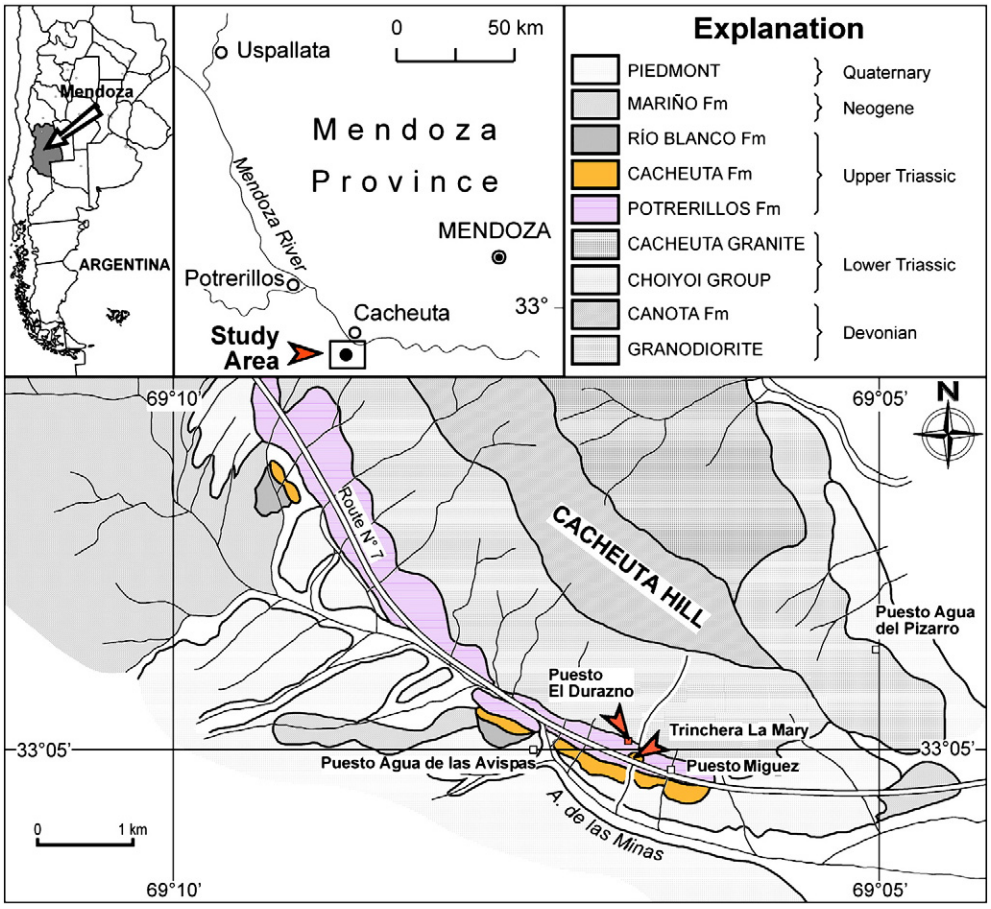

Fig. 1. Location map and geologic sketch of the sampling area (adapted from Morel, 1994).

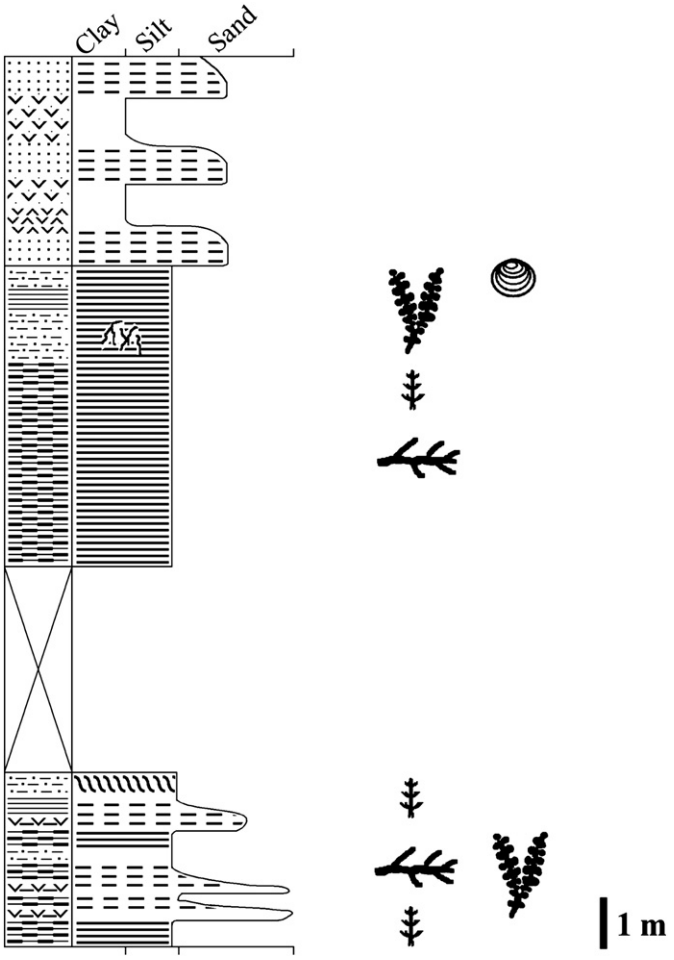

Fig. 2. Stratigraphic section of Puesto El Durazno locality, Cacheuta, Mendoza, Argentina. Legend as in Fig. 3.

remains of weakly biomineralized conchostracans are abundant and well-preserved.

(12) 400 cm of whitish tuffite, tuff and sandstone.

2.2. Trinchera La Mary locality

At Trinchera La Mary (33°04′44″ S, 69°07′11″ W, approximately 220 m to the SW of Puesto El Durazno, Fig. 1), the strike and dip changed to 105°/27° S and the ca. 4 m outcrop consists predominantly of fine-grained clastic rocks (see Fig. 3). The plant fossils are well-preserved compressions with cuticles. From the lowermost part upwards exposures are as follows:

(1) 160 cm of fine-grained, crossbedded siltstone.
(2) 12 cm of a fine-sandy (lower part) silty to argillaceous (upper part) paleosol whose uppermost 2 cm represent a rooted underclay covered by.
(3) 1 cm of a gray to brown cuticle-paper bed with an argillaceous matrix, which is overlying a coal seam ($R_0\% = 0.61 \pm 0.06$; $n = 40$) a few mm thick.
(4) 20 cm of finely laminated gray to black shale bearing abundant fossil plant material (compressions with well-preserved cuticles).
(5) 15 cm of a poorly stratified claystone with rare plant debris.
(6) 190 cm of gray, laminated shale and siltstone, with an intercalation of 17 cm of silty, fine-grained sandstone at 15 cm above the base of this unit. Following upwards are 30 cm of gray siltstone containing conchostracans and corystosperms and 115 cm of shale and siltstone. The uppermost part of the unit (6) is composed of 110 cm of gray shale, exhibiting excellently preserved plants (including cuticles) of Corystospermaceae, Peltaspermaceae and Voltziaceae as well as Euestheriidae (conchostracans).

Table 1
Sample forms used.

Sample form	Description
Fossil as preserved in rock	
(1) Compression	Conceptualized by an analog model of the anatomy of an extant leaf: "vitrinite (mesophyll) + cuticle (biomacropolymer) = compression" (Zodrow et al., 2009).
(2) Cuticle-free coalified layer	Coalified plant remain without preserved cuticle.
Derived from Schulze's process	
(3) Cuticle	Thin film of biomacropolymeric structure obtained from compression by Schulze's maceration process.
Other	
(4) Coal (vitrain)	Bright and shiny banded bituminous coal.

3. Comments on systematics

The most commonly found fossils at the collection sites include several taxa of the *Dicroidium* flora (Figs. 4, 5 and 6), which have been described in previous publications (e.g., Frenguelli, 1948; Jain and Delevoryas, 1967; Kurtz, 1921; Morel, 1994; Morel et al., 2010; Morel and Povilauskas, 2002; Stipanicic et al., 1995; Zuber, 1887), and we refrain from recounting taxonomic details. Table 2 summarizes relevant fossil-sample information and the nomenclature for each species, omitted from the text for brevity. A single, fragmentary specimen of *Linguifolium tenison-woodsii* (Etheridge) Retallack (1980) is included for comparison, which, to the best of our knowledge has not been recorded before from the Triassic of the Cacheuta Hill.

As a result of the unresolved systematics of the Corystospermaceae, two different taxonomic approaches are recognized. In the first approach, some authors employ several generic names such as *Dicroidium*, *Diplasiophyllum*, *Johnstonia*, *Xylopteris* and *Zuberia* (e.g., Artabe, 1990; Baldoni, 1980; D'Angelo, 2006; Gnaedinger and Herbst, 2001; Morel et al., 2003, 2010; Pattemore and Rigby, 2005; Petriella, 1979, 1981, 1985; Retallack, 1977; Stipanicic et al., 1995; Zamuner et al., 2001; Zodrow et al., 2009). In the second approach, some other authors synonymized all those generic names with *Dicroidium* (e.g., Abu Hamad et al., 2008; Anderson et al., 2008; Anderson and Anderson, 1983; Archangelsky, 1968; Bomfleur and Kerp, 2010; Bonetti, 1966; Holmes and Anderson, 2005; Taylor et al., 2009; Townrow, 1957).

We use the frond morphology of *Dicroidium*, *Johnstonia* and *Zuberia* according to the taxonomic guidelines given by Retallack (1977) and Petriella (1979).

4. Materials and sample preparations

Cuticle-free coalified layers from Puesto El Durazno locality are released from the silty matrix by using a scalpel and 24 M hydrofluoric acid (HF), whereas the relatively loosely attached compressions at Trinchera La Mary are removed from the rock matrix by scalpel. In a few specimens, compressions are released from the pelitic surface using 24 M HF for a few minutes.

Each compression sample is split into two portions; one is retained without further treatment, whereas the other is macerated. Maceration is carried out by immersing compressions in Schulze's solution, prepared with 5 g potassium chlorate ($KClO_3$) dissolved in 150 ml of 16 M nitric acid (HNO_3), for a maximum of 1 h. Cuticles obtained are

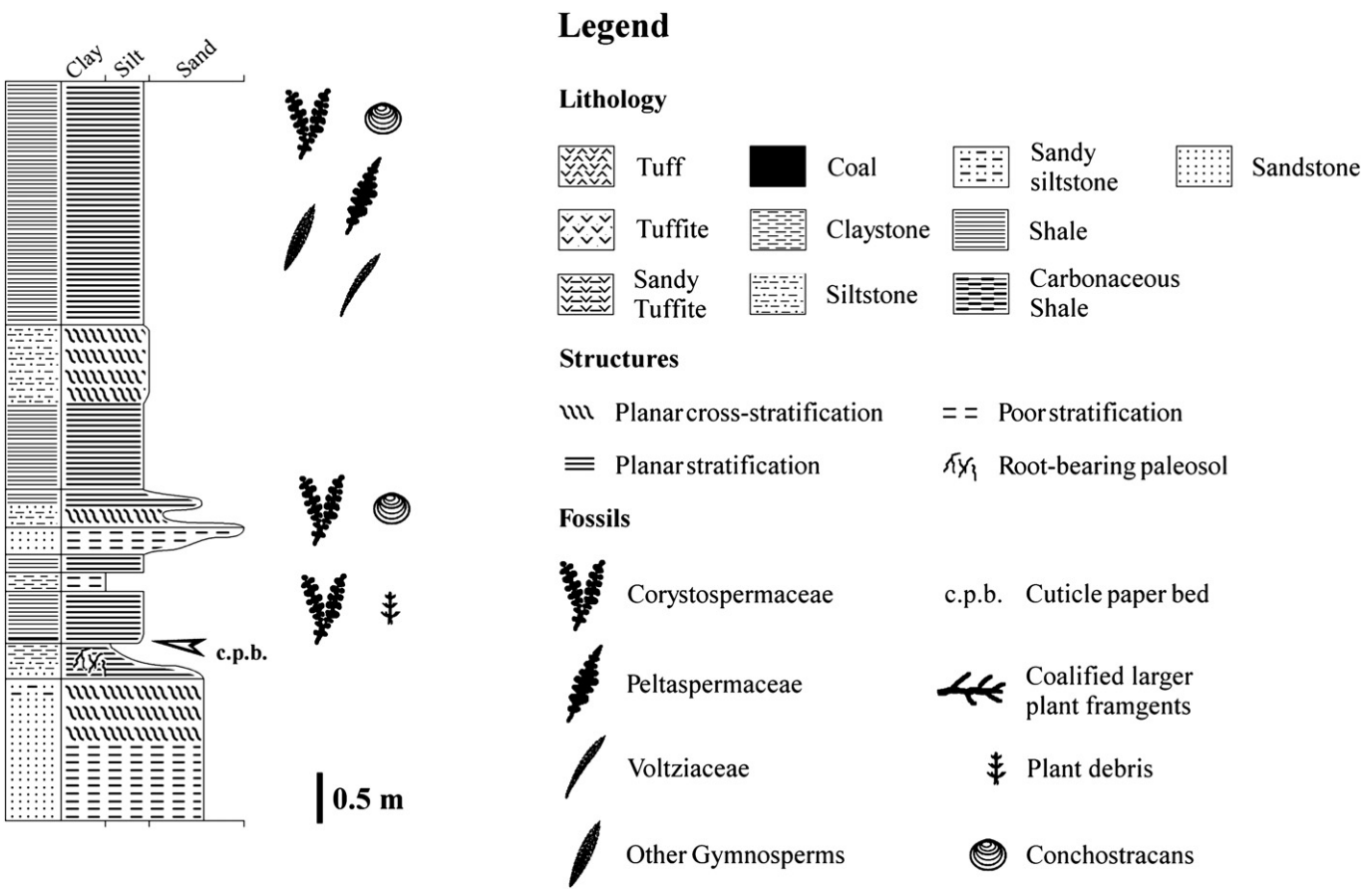

Fig. 3. Stratigraphic section of Trinchera La Mary locality, Cacheuta, Mendoza, Argentina.

treated in 1.3 M ammonium hydroxide solution (NH_4OH) and finally rinsed in distilled water.

5. Methods

5.1. Qualitative and semi-quantitative Fourier transform infrared-spectrometry analysis

Samples are analyzed utilizing potassium bromide (KBr) pellets (0.5 to 2.0 mg sample with 100 mg KBr and compressing the ground mixture into a 13-mm diameter pellet). FTIR spectra are obtained using a Nicolet "Protégé 460" Spectrometer, equipped with a CsI beamsplitter, a DTGS-CsI detector and an Ever Glo-type source. Acquisition conditions include 4 cm^{-1} resolution and 64 co-added interferograms before Fourier transformation. Spectral band assignments are made according to Painter et al. (1981), Wang and Griffiths (1985), Ingle and Crouch (1988), and Colthup et al. (1990).

Semi-quantitative FTIR analysis includes infrared (IR) absorbance-peak area determinations and calculations of area ratios (see Table 3 for definition and interpretations of semi-quantitative IR-derived ratios). Area-integration methods used are according to Sobkowiak and Painter (1992); Mastalerz and Bustin (1993a); Lis et al. (2005) and D'Angelo (2004, 2006). The methylene/methyl (CH_2/CH_3) ratio is calculated after Fourier self-deconvolution of the aliphatic stretching region (3000–2800 cm^{-1}) into individual peaks (see Lin and Ritz, 1993a,b and Zodrow and Mastalerz, 2007, p. 320). Areas of $-CH_2$ bands at 2925 cm^{-1} plus 2853 cm^{-1} are divided by the sum of two areas of $-CH_3$ bands at 2958 cm^{-1} and 2875 cm^{-1} to obtain the CH_2/CH_3 ratio.

For comparison of IR-derived ratios within and between species, a consistent determination of band-region endpoints is essential (Zodrow and Mastalerz, 2007).

5.2. Strategy of principal component analysis (PCA) for FTIR-derived data

Reduction of dimensionality of a data set consisting of a large number of variables is the central idea of PCA, a nonparametric, pattern-recognizing method, which at the same time retains as much as possible of the variation present in the data set. Principal components (PCs) are assumed uncorrelated (orthogonal) and ordered in decreasing magnitude of explained variance (Anderson, 2003; Izenman, 2008; Johnson and Wichern, 2007; Jolliffe, 2002; Lattin et al., 2002; Rencher, 2002). We retain components whose cumulative explained variance is close to 90% (Kaiser, 1960; see Kendall, 1965 for other methods).

The larger number of data points (328: forty-one samples and eight attributes, Table 4) provides an opportunity for PCA to focus on grouping data as a function of chemical structure (i.e., functional groups). This is designated PCA[A]. A second principal component analysis, PCA[B], is performed based on only the twenty-nine coaly sample forms (i.e., compressions, cuticle-free coalified layers and coals), and four attributes, viz. CH_2/CH_3, Al/Ox, 'A' factor and 'C' factor. PCA is performed using STATISTICA® (StatSoft Inc, 2001).

6. Results and discussion

6.1. FTIR qualitative analysis

Visual inspection of FTIR spectra of plant remains and associated coals shows similar general characteristics, indicating the presence of

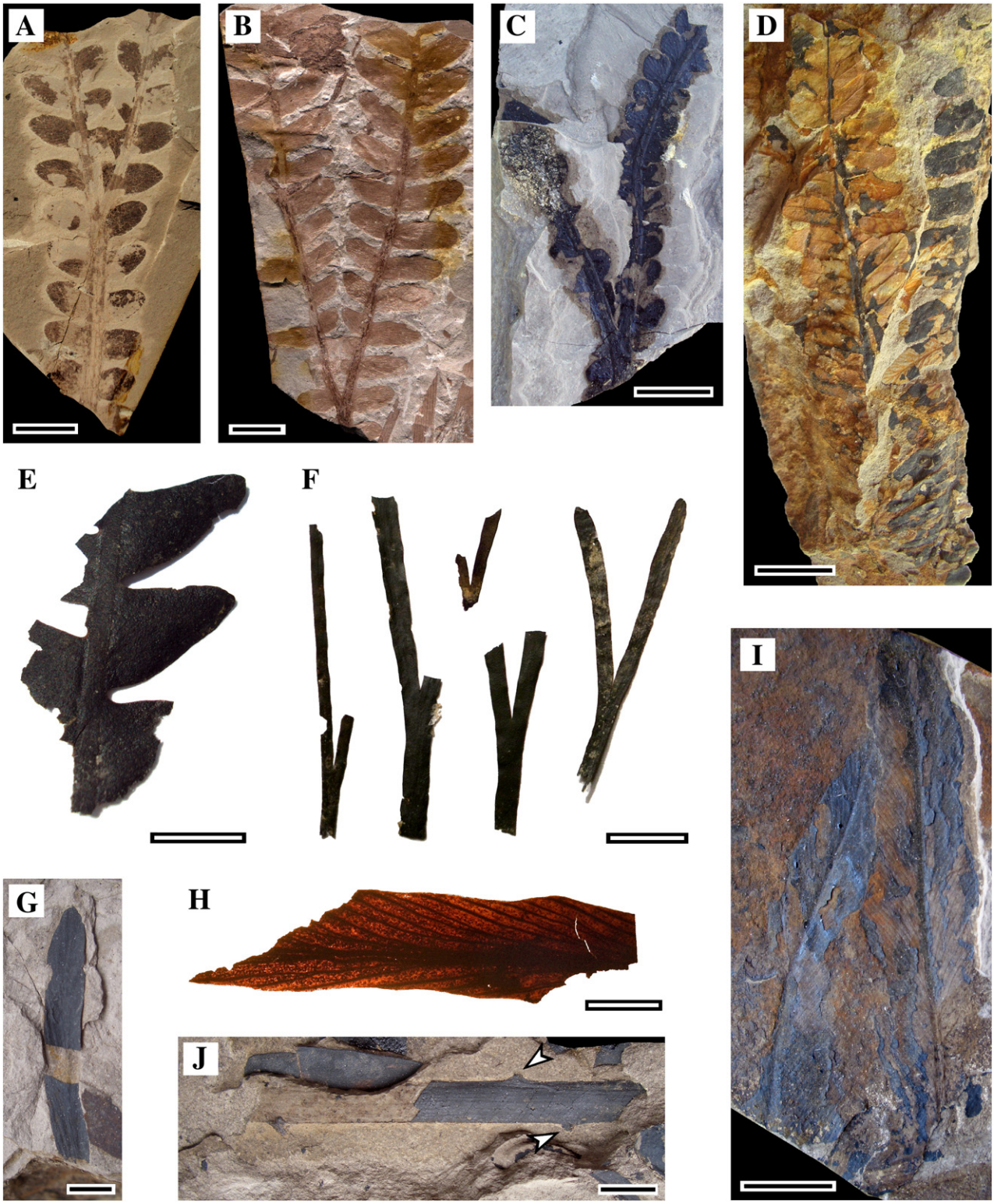

Fig. 4. Hand specimens from Puesto El Durazno (A–B) and Trinchera La Mary localities (C–J) showing different taxa and preservation modes. *Dicroidium odontopteroides*: (A) and (B) cuticle-free coalified layers, (C) compression, and (E) detached compression. *Kurtziana* sp.: (D) compression. *Johnstonia coriacea*: (F) detached compressions showing the leaf fork. *Heidiphyllum elongatum*: (G) compression. *Linguifolium tenison-woodsii*: (H) compression photographed using transmitted light. *L. Steinmannii*: (I) compressions. Indeterminate axis: (J) compression of a likely seed fern axis; arrows indicate fragmentary rachides. Scale bars: A, B, C, D, E, F, I = 10 mm; G, H, J = 5 mm.

similar functional groups in their chemical structure. Thus, only selected FTIR spectra are shown in Figs. 5, 6 and 7. Unless otherwise indicated, peak assignments are general and applicable to all of the types of samples here studied.

A broad and intense band centered between 3433 and 3200 cm^{-1} and generally attributed to H-bonded hydroxyl (OH) stretch in alcohols and phenols is shown by all of the sample forms (Figs. 5, 6 and 7).

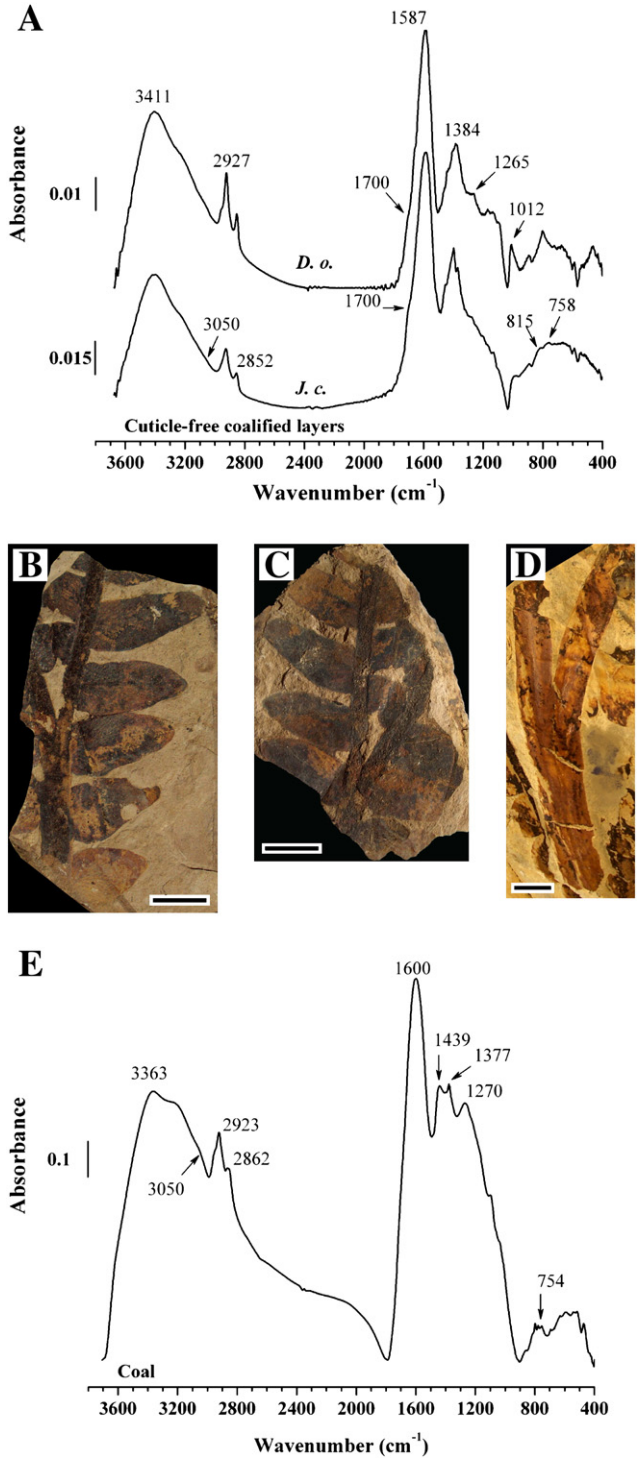

Fig. 5. Cuticle-free coalified layers, Puesto El Durazno locality. (A) FTIR spectra of *D. odontopteroides* — *D. o.* — (B and C: part and counterpart, respectively) and *J. coriacea* — *J. c.* — (D). Scale bars: B, C = 10 mm, and D = 5 mm. (E) FTIR spectra of Cacheuta coal.

A barely detectable band centered at 3050 cm^{-1} is assigned to aromatic C–H stretching vibrations. This band is absent in cuticles only.

Distinct peaks, assigned to aliphatic C–H stretching vibrations, are present in the region 3000–2800 cm^{-1}. These bands are assigned to anti-symmetric methylene (CH_2) stretch (2936–2916 cm^{-1}) and symmetric CH_2 stretch (2863–2843 cm^{-1}) (Colthup et al., 1990; Shurvell, 2002 and Stuart, 2004).

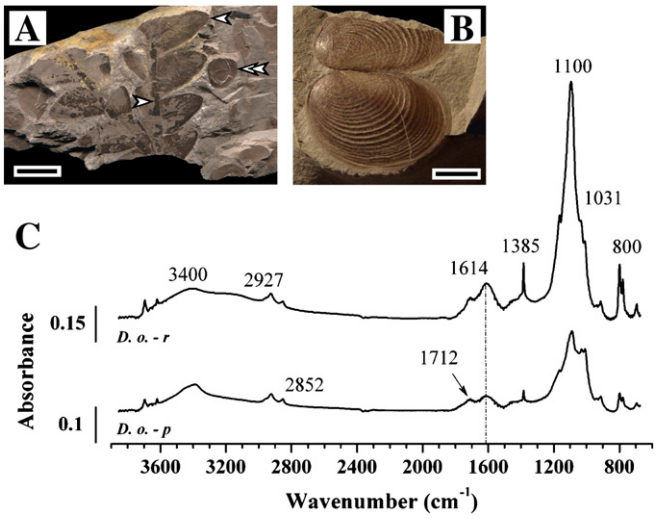

Fig. 6. Cuticle-free coalified layers, Puesto El Durazno locality. (A) Co-occurring specimens of *Euestheria forbesi* (double arrow) and *D. odontopteroides* (arrows indicate sampling zones). (B) Well-preserved specimen of *E. forbesi* showing nearly complete valves of the carapace. Scale bars: A = 10 mm; B = 5 mm. (C) FTIR spectra of *D. odontopteroides* pinnule (*D. o.* — *p*) and *D. odontopteroides* rachis (*D. o.* — *r*).

Depending on sample forms different absorptions are recorded in the region 1800–1000 cm^{-1}. Weak absorptions (shoulders) at ~1700 cm^{-1} due to carbonyl (C═O) stretching of carboxyl and other C═O groups (e.g., singly conjugated ketones) are exhibited by compressions (Fig. 7A, C and E). Cuticles show distinct bands at higher wavenumbers (1708 cm^{-1} and 1714 cm^{-1}) which could be indicative of acids or ketones (Fig. 7B, D and F).

A broad and intense peak centered at 1618–1587 cm^{-1} (compressions, cuticle-free coalified layers and coal samples), and at 1645–1639 cm^{-1} (cuticle samples) is the result of the contribution of several structures: aromatic, olefinic, quinoid, ketone and, to some extent, conjugated carbonyl and some amide groups (Figs. 5A and E and 7A to F).

Table 2
Nomenclature and fossil-sample information.

Nomenclature	Sample analyzed	Sample form[c]
Corystospermaceae (seed fern)		
Dicroidium odontopteroides (Morris) Gothan (1912)	Pinnule, no rachis	Comp Cuticle CL
	Rachis	CL
Johnstonia coriacea (Johnston) Walkom (1925)	Leaf	Comp Cuticle CL
Zuberia feistmanteli (Johnston) *Frenguelli emend.* Artabe (1990)	Pinnule, no rachis	CL
Voltziaceae (conifer)		
Heidiphyllum elongatum (Morris) Retallack (1981) [a]	Leaf	Comp
Zamiaceae (cycad-related?)		
Kurtziana sp. [b]	Leaf	Comp Cuticle
Gymnospermopsida incertae sedis		
Linguifolium tenison-woodsii (Etheridge) Retallack (1980) [a]	Leaf	Comp
L. steinmannii (Solms-Laubach) Frenguelli (1941) [a]	Leaf	Comp
Indeterminate axis	Axis	Comp

[a] The cuticle could not be obtained.
[b] Because of fragmentary preservation, studied specimen is classified only to the generic level.
[c] Comp = Compression (see Table 1), CL = Cuticle-free coalified layer.

Table 3
Definition and interpretation of IR-derived, semi-quantitative ratios employed in this study.

Ratio	Band-region (cm^{-1})	Interpretation and remarks
	Band-region ratios	
CH_2/CH_3	3000–2800	Methylene/methyl ratio. This ratio relates to the aliphatic chain length and to the degree of branching of aliphatic side groups (side chains attached to the macromolecular structure) (Lin and Ritz, 1993a, b). *Interpretation*: A larger ratio implies comparatively longer and straight chains, a smaller ratio shorter and more branched chains.
Al/Ox	(3000–2800)/(1800–1600)	Aliphatic/Oxygen-containing compounds ratio. Relative contribution of aliphatic C–H stretching bands (Al) to the combined contribution of oxygen-containing groups and aromatic carbon (Ox). *Interpretation*: From larger ratios decreasing oxygen-containing groups can be inferred, or the lower the Al/Ox ratio, the higher the Ox term.
Al/C═C	(3000–2800)/(1600–1500)	Aliphatic/aromatic carbon groups ratio. Relative contribution of aliphatic C–H stretching bands to aromatic carbon groups (C═C). *Interpretation*: Larger ratios indicate increasing aliphatic groups to aromatic carbon groups. This ratio is equivalent to the I1 index of Guo and Bustin (1998).
C═O/C═C	(1700–1600)/(1600–1500)	Carbonyl/aromatic carbon groups ratio. Relative contribution of carbonyl/carboxyl groups (C═O) to aromatic carbon groups. *Interpretation*: Larger ratios indicate increasing carbonyl/carboxyl groups to aromatic carbon groups.
C═O cont	(~1714)/(1800–1600)	Carbonyl contribution. Relative contribution of carbonyl/carboxyl groups (C═O, peak centered near 1714 cm^{-1}) to the combined contribution of oxygen-containing groups and aromatic carbon (C═C) structures.
C═C cont	(~1600)/(1800–1600)	Aromatic carbon contribution. Relative contribution of aromatic carbon groups (C═C, peak in the region 1650 to 1520 cm^{-1} and centered near 1600 cm^{-1}) to the combined contribution of oxygen-containing groups and aromatic carbon (C═C) structures.
'A' factor = Al/(Al + C═C)	(3000–2800)/[(3000–2800) + (1650–1520)]	'A' factor. Relative contribution of aliphatic C–H stretching bands to the summation of aliphatic C–H stretching and aromatic carbon structures. *Interpretation*: according to Ganz and Kalkreuth (1987) it represents changes in the relative intensities of the aliphatic groups.
'C' factor = Ox/(Ox + C═C)	(1800–1600)/[(1800–1600) + (1650–1520)]	'C' factor. Relative contribution of oxygen-containing compounds to the summation of oxygen-containing structures and aromatic carbon bands. *Interpretation*: according to Ganz and Kalkreuth (1987) it represents changes in the carbonyl/carboxyl groups.

Some cuticles show a small peak at 1558 cm^{-1} that could tentatively be assigned to amide structures (Fig. 7B and D).

In all the sample forms, aliphatic (alkyl) C–H deformations are represented by medium intensity peaks at 1456 cm^{-1} and 1439 cm^{-1} (e.g., Figs. 5E and 7A) assigned to either CH_3 anti-symmetric or CH_2 scissor deformation. Medium intensity peaks centered at 1398–1377 cm^{-1} (e.g., Figs. 5E and 7C and E) represent different alkyl C–H vibrations assigned to CH_3 umbrella deformation (see Gauglitz and Vo-Dinh, 2003, p. 99 for definitions of CH_2 and CH_3 group vibrations).

The broad band at 1278–1265 cm^{-1} could be assigned to methoxyphenolic, lignin-derived aromatic units (Durig et al., 1988 and Zodrow et al., 2000).

Bands at 1100 cm^{-1}, 1031 cm^{-1} and 800 cm^{-1} are attributed to Si–O stretching (silicate impurities, Fig. 6C).

Weak bands near 1012 cm^{-1} (spectra of cuticle-free coalified layers) are usually assigned to aromatic C–H in-plane bending vibrations (on a benzene ring, Fig. 5A, *D. o.*) which are characteristically absent in cuticle spectra.

Low intensity bands that occur in the region 900–700 cm^{-1} are of special interest in evaluating sample forms. For example, in compression and in samples of cuticle-free coalified layer these bands occur at 870 cm^{-1}, 825 cm^{-1}, 815 cm^{-1}, 758,cm^{-1}, 755 cm^{-1} and 750 cm^{-1}, and are assigned to aromatic C–H out-of-plane bending vibrations (Figs. 5A and 7A and C). Coal samples show similar peaks in this region (e.g., at 754 cm^{-1}, Fig. 5E), indicating similarities in the aromatic structure. In contrast, cuticles rarely show aromatic bands in this region. Instead, there are some bands at 848 cm^{-1} that could tentatively be assigned to CH_2 vibrational modes (Fig. 7B, D and F; compare with Fig. 8C of Zodrow and Mastalerz, 2001).

6.2. Semi-quantitative comparison with kerogen types and coal macerals

Differences with respect to functional groups within the different sample forms are semi-quantified by IR data (Table 4) that are basic to investigating maturity levels and chemical similarity with kerogen types and coal macerals. Our semi-quantitative IR data from all the sample forms are compared with some available IR data from coal macerals (Guo and Bustin, 1998; Mastalerz and Bustin, 1996) with approximately the same rank ($R_{0\ max}$ 0.52%–1.41%). All the sample forms are shown in a diagram of 'A' vs. 'C' factors (as defined by Ganz and Kalkreuth, 1987), similar to the traditional van Krevelen H/C–O/C plot (Fig. 8), indicating similarities with different types of kerogen. Band areas (not peak intensities) are used in this study to calculate 'A' and 'C' factors. The 'A' factor represents changes in the relative intensities of the aliphatic groups and the 'C' factor represents changes in the carbonyl groups (see Table 3 for definitions). Fig. 9 is a simplified plot of Fig. 8 indicating the approximate regions of the different sample forms studied (ellipses around the groups are used for clarity only). In this case, the reorganization of the carbon skeleton as a function of kerogen types is indicated by generalized molecular structures.

A more comprehensive evaluation of the complete data set (semi-quantitative FTIR data in Table 4) is carried out by means of PCA in Section 6.3.

6.2.1. Compressions

All the compression-preserved taxa are similar in composition to some resinite and sporinite coal macerals, (Fig. 8), but that of *Kurtziana* sp. (Fig. 4D) is somewhat different. The latter has notably higher values of the 'C' factor, therefore showing similarities to some bituminite macerals and cuticles (Figs. 8 and 9). This probably reflects the contribution from a relatively thick cuticle characterizing *Kurtziana*. Previous cuticular studies led to the inference of a xeromorphic taxon (*K. brandmayri* Frenguelli; Artabe et al., 1991).

Compressions of all taxa are Type II kerogen, showing high 'A' factor values and lower 'C' factors, which could be interpreted as being a relatively high contribution of aliphatic groups and lower contents of oxygen-containing compounds, respectively. Very similar 'A' and 'C' factor values are exhibited by compressions of *D. odontopteroides* (Fig. 4C and E), *J. coriacea* (Fig. 4F), *H. elongatum* (Fig. 4G) and *L. steinmannii* (Fig. 4I).

Interesting to note is that the compression specimen of *L. tenisonwoodsii* (Fig. 4 H) is Type I kerogen in the 'A' vs. 'C' factors plot (Figs. 8 and 9) as it is characterized by a comparatively high content of aliphatic compounds among the entire compression-sample set (see 'A' factors in

Table 4
Semi-quantitative FTIR data relating to compression, cuticle-free coalified layer, cuticle, and coal samples.

Sample	Locality [a]	Taxon	Sample form [b]	CH_2/CH_3	Al/Ox	C═O/C═C	C═O cont	C═C cont	Al/C═C	'A' factor	'C' Factor
1	TLM	*Dicroidium odontopteroides*	Comp	3.8	0.88	0.2	0.05	0.25	3.53	0.78	0.17
2	TLM	*D. odontopteroides*	Comp	3.3	0.62	0.2	0.04	0.19	3.36	0.77	0.18
3	TLM	*D. odontopteroides*	Comp	4.9	0.96	0.3	0.06	0.21	4.50	0.82	0.23
4	TLM	*D. odontopteroides*	Comp	2.4	0.52	0.08	0.02	0.26	1.99	0.67	0.07
5	TLM	*D. odontopteroides*	Comp	3.2	0.55	0.2	0.05	0.21	2.69	0.73	0.18
6	TLM	*D. odontopteroides*	Comp	2.5	0.52	0.08	0.02	0.26	2.01	0.67	0.07
7	TLM	*Johnstonia coriacea*	Comp	3.6	0.41	0.2	0.03	0.13	3.08	0.75	0.17
8	TLM	*J. coriacea*	Comp	3.7	0.47	0.3	0.04	0.17	2.77	0.74	0.20
9	TLM	*J. coriacea*	Comp	3.7	0.56	0.2	0.03	0.20	2.75	0.73	0.14
10	TLM	*J. coriacea*	Comp	3.7	0.54	0.2	0.03	0.13	4.17	0.81	0.17
11	TLM	*J. coriacea*	Comp	3.0	0.62	0.1	0.03	0.25	2.46	0.71	0.12
12	TLM	*Heidiphyllum elongatum*	Comp	4.6	0.93	0.2	0.04	0.24	3.90	0.80	0.15
13	TLM	*Linguifolium tenison-woodsii*	Comp	4.9	1.14	0.2	0.05	0.22	5.14	0.84	0.19
14	TLM	*L. steinmannii*	Comp	2.6	0.66	0.1	0.03	0.24	2.73	0.73	0.11
15	TLM	*Kurtziana* sp.	Comp	2.3	0.35	6	0.3	0.05	7.10	0.88	0.85
16	TLM	Indeterminate axis	Comp	1.5	0.50	0.05	0.01	0.25	1.98	0.66	0.04
17	TLM	*D. odontopteroides*	Cuticle	9.0	0.89	5.3	0.3	0.05	16.54	0.94	0.84
18	TLM	*D. odontopteroides*	Cuticle	8.7	1.04	6.1	0.3	0.05	22.83	0.96	0.86
19	TLM	*D. odontopteroides*	Cuticle	8.0	0.98	6.1	0.3	0.05	21.78	0.96	0.86
20	TLM	*D. odontopteroides*	Cuticle	6.3	1.18	3.0	0.2	0.07	17.09	0.94	0.75
21	TLM	*D. odontopteroides*	Cuticle	11.7	1.09	2.7	0.2	0.07	15.00	0.94	0.73
22	TLM	*J. coriacea*	Cuticle	7.6	0.78	2.0	0.2	0.08	9.74	0.91	0.67
23	TLM	*J. coriacea*	Cuticle	7.1	0.58	1.7	0.1	0.08	6.82	0.87	0.63
24	TLM	*J. coriacea*	Cuticle	7.1	0.89	2.8	0.2	0.06	14.42	0.94	0.74
25	TLM	*J. coriacea*	Cuticle	8.4	0.87	7.1	0.3	0.04	21.92	0.96	0.88
26	TLM	*J. coriacea*	Cuticle	11.7	0.92	1.6	0.2	0.09	9.80	0.91	0.62
27	TLM	*Kurtziana* sp.	Cuticle	6.3	1.14	5.3	0.3	0.05	23.04	0.96	0.84
28	PED	*D. odontopteroides*	CL	2.3	0.14	0.08	0.02	0.30	0.48	0.32	0.07
29	PED	*D. odontopteroides*	CL	4.7	0.16	0.1	0.04	0.29	0.55	0.35	0.12
30	PED	*D. odontopteroides*	CL	3.0	0.15	0.08	0.02	0.27	0.55	0.36	0.08
31	PED	*D. odontopteroides*	CL	3.0	0.07	0.03	0.01	0.43	0.16	0.14	0.03
32	PED	*D. odontopteroides*	CL	3.5	0.18	0.01	0.004	0.45	0.39	0.28	0.009
33	PED	*D. odontopteroides*	CL	3.1	0.41	0.07	0.02	0.25	1.65	0.62	0.061
34	PED	*D. odontopteroides*-pinnule	CL	3.3	0.34	0.3	0.06	0.19	1.73	0.63	0.23
35	PED	*D. odontopteroides*-rachis	CL	3.3	0.21	0.1	0.03	0.25	0.86	0.46	0.11
36	PED	*J. coriacea*	CL	5.1	0.12	0.03	0.02	0.45	0.27	0.21	0.033
37	PED	*Zuberia feistmanteli*	CL	3.5	0.14	0.07	0.04	0.53	0.27	0.21	0.067
38	TLM	Coal 1	Vitrain	1.7	0.17	0.00005	0.000009	0.18	0.95	0.49	0.00005
39	TLM	Coal 2	Vitrain	1.8	0.18	0.0003	0.00007	0.24	0.77	0.44	0.0003
40	TLM	Coal 3	Vitrain	1.2	0.15	0.02	0.004	0.25	0.58	0.37	0.016
41	TLM	Coal 4	Vitrain	1.1	0.13	0.02	0.006	0.28	0.46	0.32	0.021

[a] TLM = Trinchera La Mary; PED = Puesto El Durazno.
[b] Comp = compression; CL = Cuticle-free coalified layer.

Table 4). The specimen seems to be naturally macerated, its appearance resembling that of the fossilized cuticles of *Alethopteris ambigua* (Lesquereux) *pars* (Zodrow and Cleal, 1998) from the Pennsylvanian of the Sydney Coalfield, Nova Scotia, Canada. More importantly, many similarities exist regarding functional groups between *L. tenison-woodsii* (from Cacheuta) and *A. ambigua* (from Sydney), as is evident from the 'A' vs. 'C' factors plots (see *A. ambigua* in Fig. 8 of D'Angelo et al., 2010). *L. tenison-woodsii* shows the highest CH_2/CH_3 values among the compression-form samples (Table 4), i.e., more similar to the cuticle form. Fossilized-cuticle formation is not yet completely understood, though it is partly thermo-dependent and partly generated by in situ maceration (i.e., pyritic oxidation) of compressions as proposed by Zodrow and Mastalerz (2009).

Remains of one indeterminate axis (Fig. 4J) included for comparisons with the foliage show a particularly low CH_2/CH_3 value. This indicates comparatively shorter and more branched polymethylenic side chains, very similar to those of coals (Table 4). Other similarities between the axis and coals can be seen in the low content of carbonyl compounds (low values of C═O cont and 'C' factor).

With the exception of a few samples, compressions, coal samples and coal macerals (mainly vitrinite) shared a similar thermal history, as inferred from similarities in some of their functional groups such as similar distributions and similar relative contents (e.g., 'A' factor and 'C' factor). This is considered as additional support for our previous statements regarding compressions as being mini coal seams (Zodrow et al., 2009) with a composition similar to that of some coals and coal macerals (i.e., resinites and sporinites).

6.2.2. Cuticle-free coalified layers

They were found only at Puesto el Durazno locality (Figs. 5B–D and 6A), and are characterized by relatively medium to low values of the 'A' and of the 'C' factors thereby revealing medium to low contributions from aliphatic and oxygen-containing compounds, respectively. Most of the cuticle-free coalified layers are Type III kerogen and similar in composition to some vitrinites and coal samples. Spectra of *D. odontopteroides* and *J. coriacea* (Fig. 5A) resemble those of coal (Fig. 5E). Here only a few functional groups are left accounting for a simple chemical structure, which is in agreement with cuticle-free coalified layers reported by Zodrow et al. (2009) for the Triassic of Cacheuta.

One pinnule (Fig. 6C, lower spectrum) and its relatively highly coalified rachis above the main fork of a specimen of *D. odontopteroides* (Fig. 6A) were separately analyzed, and are Type II kerogen. But comparisons of their IR data indicate the higher aromatic character of the rachis, e.g., lower values of 'A' and 'C' factors and C═O/C═C (Table 4). This is shown by 'A' vs. 'C' factors plot (Fig. 8) where the rachis specimen is located closer to coal samples and cuticle-free coalified layers. The pinnule is more similar to cutinites and compressions, exhibiting a comparatively more aliphatic composition.

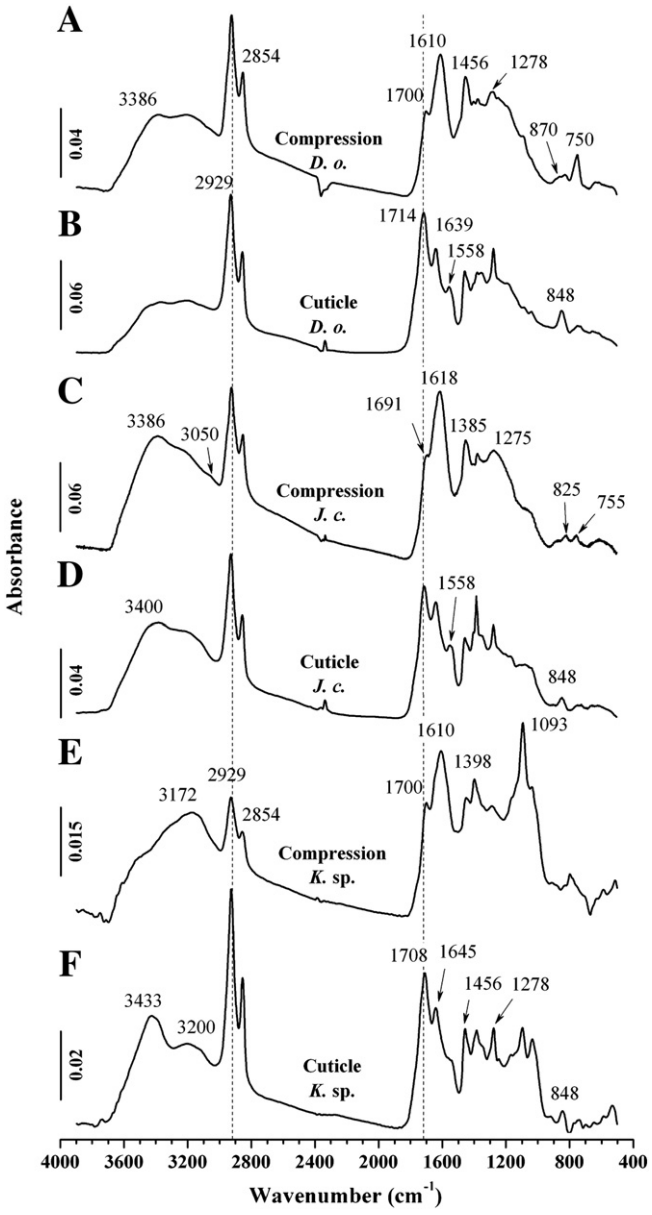

Fig. 7. FTIR spectra of compressions and cuticles. (A) and (B) *D. odontopteroides* (*D. o.*). (C) and (D) *J. coriacea* (*J. c.*). (E) and (F) *Kurtziana* sp. (*K.* sp.).

Chemical differences between compressions (Trinchera La Mary locality) and cuticle-free coalified layers (Puesto el Durazno locality) in terms of IR-derived ratios, likely reflect differing diagenetic and post-diagenetic influences (Table 4). Cuticle-free coalified layers show lower contributions of oxygen-containing groups (e.g., carbonyls) than compressions (see Table 4 and compare Figs. 5A and 7A). Furthermore, it is suggested that the cuticle-free coalified layers of corystosperms particularly resemble vitrinite (kerogen type III, Mastalerz and Bustin, 1993b, Fig. 4), as they have dominant aromatic carbon bands (high intensity peak at ca. 1587 cm^{-1}, Fig. 5A), and smaller aliphatic contributions in the 3000–2800 cm^{-1} region.

6.2.3. Cuticles

They are characterized by high values of both 'A' and 'C' factors, indicating high contents of aliphatic and oxygen-containing compounds, respectively. In general, cuticles of *D. odontopteroides* and *Kurtziana* sp. show somewhat higher values of 'C' factors than *J. coriacea*. CH_2/CH_3 values recorded for all the cuticles are higher than those of the other sample forms (i.e., compressions, cuticle-free coalified layers, and coals). This implies comparatively longer and less branched aliphatic structures.

Comparisons indicate that cuticles have a composition similar to some coal macerals, viz. alginite, bituminite and cutinite (Figs. 8 and 9). All the taxa are located (approximately) at the boundary between kerogen Types I and II in the 'A' vs. 'C' factors plot (Fig. 8), where linear or branched hydrocarbons and some cyclic compounds are dominant (Fig. 9).

The more salient functional groups of cuticles indicate a signature characteristic of the biomacromolecules cutan/cutin, i.e., a high-aliphatic character, the carbonyl content, the length and branching of the polymethylenic chains and the absence of aromatic C–H bands (e.g., Gupta et al., 2007; Logan et al., 1993; Nip et al., 1986a,b; Tegelaar et al., 1991; van Bergen et al., 2004; Zodrow et al., 2000, 2009).

6.3. Principal component analysis

6.3.1. PCA[A] of all the sample forms

A solution of two components accounting for 89.2% of the variance is acceptable in spite of the sharp drop in eigenvalue from 6.37 to 0.76, which assumes that the second component is not merely a mathematical construct but an estimator of the population component (Kendall, 1965). The loading plots and scores are shown in Figs. 10 and 11, respectively. Fig. 12 is a simplified plot where the groupings of the sample forms are indicated by delimiting ellipses around the groups, which are for clarity only.

The first component (79.7% explained variance) involves mainly negative loadings, except for the positive loading on C═C cont (aromatic carbon contribution), which highlights the presence of aromatic carbon groups vs. the other functional groups. Cuticles exhibit the most negative scores (Fig. 11, x axis), reflecting their low content of aromatic carbon groups and their highly aliphatic nature. This is clearly shown by the lowest C═C cont values and the high values of both Al/C═C and 'C' factor (Table 4). It is particularly the case of most cuticles of *D. odontopteroides* and *Kurtziana* sp. Many cuticles of *J. coriacea* show moderate negative scores (Fig. 11, x axis).

The second component (9.5%) is mainly positive except for the moderate negative loading on C═O/C═C. Compressions show positive scores against this component (Fig. 11, y axis), as a result of the Al/Ox values being among the highest in the entire sample set (Table 4).

Cuticle-free coalified layers and coal samples exhibit negative scores against the second component, forming a tight group on the scores plot. A further distinction between them is achieved by PCA[B] (see Section 6.3.2).

The different grouping of data as a function of chemical structure shown by the plot of scores (Fig. 11) reflects the nature of the different sample forms. The group representing compressions is separated from the other groups (Fig. 12), showing an intermediate position between cuticles and cuticle-free coalified layers. The only exception is the *Kurtziana* sp. compression that shows functional groups similar to those of cuticles which is clearly evident from the highest values of both C═O/C═C and C═O cont.

Cuticle-free coalified layers represent remains of the mesophyllous component of foliage, but at a relatively higher maturity level than the compressions. Results are in agreement with our previous observations indicating the capacity of cuticle-free coalified layers to survive harsh post-diagenetic influences (Zodrow et al., 2009). Cuticle-free coalified layers represent an extreme case in the fossil preservation continuum, having functional groups similar to those of coal samples (Fig. 12).

At the other extreme, the preservation of cuticles demonstrates their higher capacity to withstand oxidizing geochemical conditions. This is exemplified as well by the existence of cuticle-paper coal at the Trinchera La Mary locality (D'Angelo et al., in prep.) that is

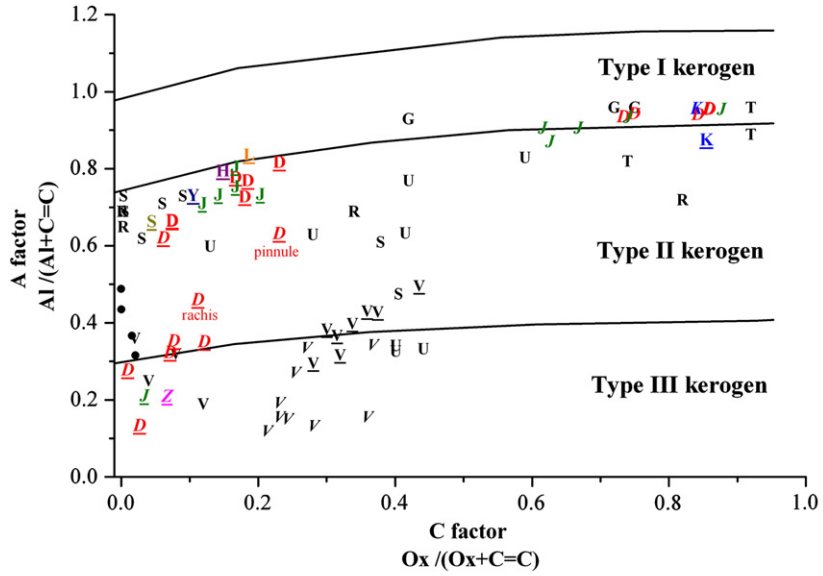

Legend

Samples (this study)

- D *D. odontopteroides* - Compression
- D *D. odontopteroides* - Cuticle
- D *D. odontopteroides* - Cuticle-free coalified layer
- J *J. coriacea* - Compression
- J *J. coriacea* - Cuticle
- J *J. coriacea* - Cuticle-free coalified layer
- Z *Z. feistmanteli* - Cuticle-free coalified layer
- K *Kurtziana* sp. - Compression
- K *Kurtziana* sp. - Cuticle
- H *H. elongatum* - Compression
- L *L. tenison-woodsii* - Compression
- Y *L. steinmannii* - Compression
- S Indeterminate axis - Compression
- • Coal

Coal macerals (literature)

- G Alginite
- V Vitrinite
- V Vitrinite - Medium volatile bituminous coal
- V Vitrinite - High volatile bituminous coal
- S Sporinite
- U Cutinite
- R Resinite
- T Bituminite

Fig. 8. Kerogen-type diagram of the sample forms and some coal macerals according to variables obtained from infrared spectra. Sources of coal maceral IR data: Mastalerz and Bustin (1996; cutinite, vitrinite of medium volatile bituminous coals and vitrinite of high volatile bituminous coals), and Guo and Bustin (1998; cutinite, resinite, bituminite, alginite and vitrinite).

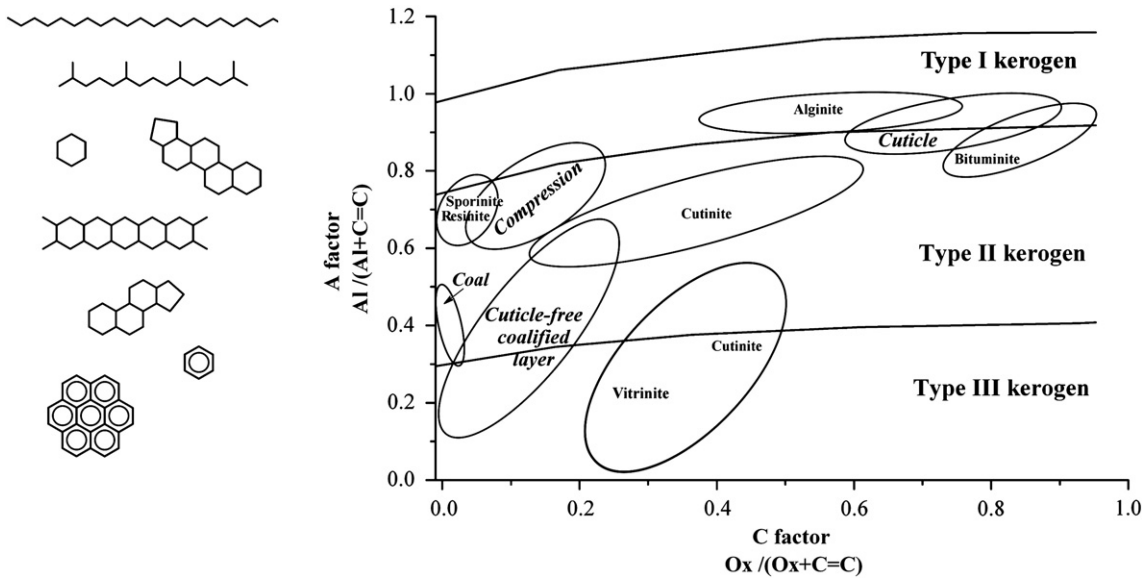

Fig. 9. Simplified plot of Fig. 8 indicating approximate regions of different sample forms (ellipses around the groups do not have any statistical significance). Carbon skeleton reorganization as a function of kerogen types is indicated by generalized structures on the left.

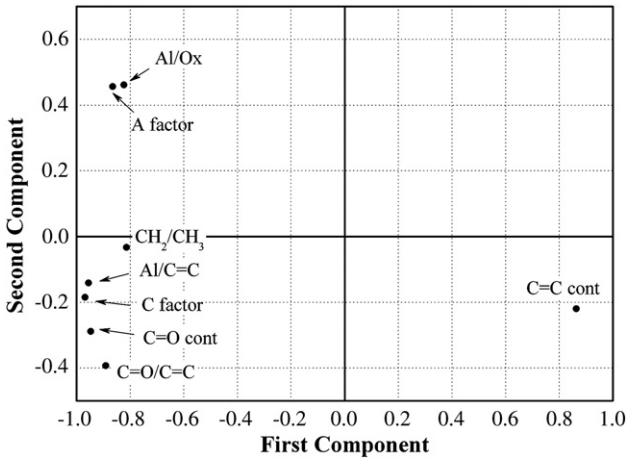

Fig. 10. Principal component analysis[A]: plot of component loadings.

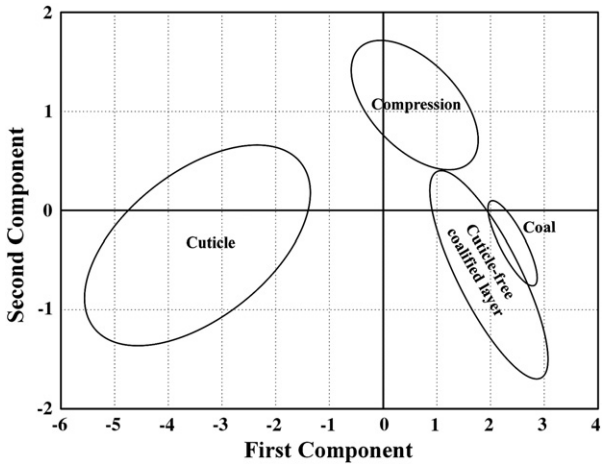

Fig. 12. Simplified plot showing groupings of fossil-derived data as indicated by approximate delimited elliptical zones that do not have any statistical significance.

morphologically and chemically similar to fossilized cuticles (see Zodrow et al., 2009). The occurrence of cuticle-paper coal is considered an index of strong acidic conditions (lower pH levels; Zodrow and Mastalerz, 2009).

Fossil preservation is related to maturation levels, geochemical factors and possibly lithology. In the stratigraphic section studied of Trinchera La Mary favorable coalification conditions prevailed (as indicated by R_0% of 0.61 at the point of sampling the coal seam; Fig. 3), allowing the preservation of compressions and their cuticles. The fine-grained lithology entombing compressions may have played a role as well in their preservation (e.g., Miltner and Zech, 1998). This combination of factors (maturation history, geochemistry and lithology) forms the background for the preservation of optimal paleophytochemical information and a high degree of biochemical fidelity (Niklas and Giannasi, 1978) could be expected.

Because of the limitations imposed by the number of specimens of each taxon available for analysis, it is too early to judge the chemotaxonomic value of PCA results, i.e., the usefulness of the score

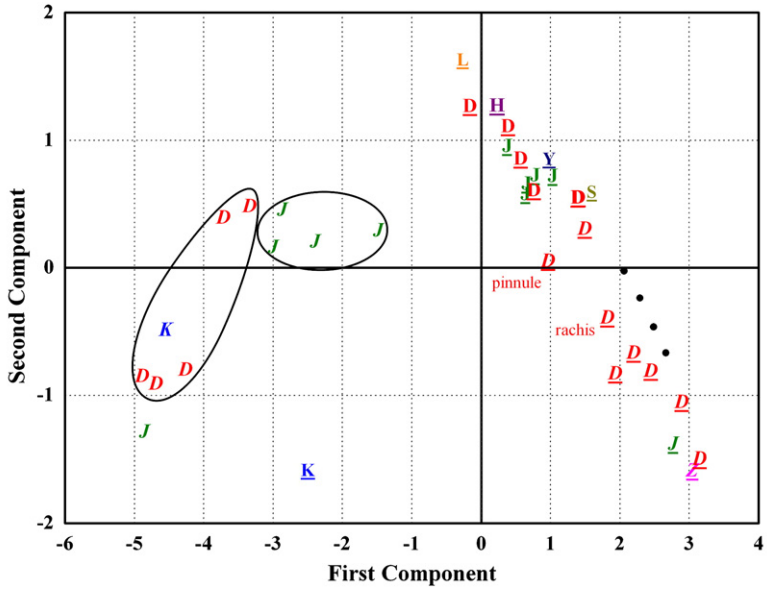

Legend

- D *D. odontopteroides* - Compression
- D *D. odontopteroides* - Cuticle
- D *D. odontopteroides* - Cuticle-free coalified layer
- J *J. coriacea* - Compression
- J *J. coriacea* - Cuticle
- J *J. coriacea* - Cuticle-free coalified layer
- Z *Z. feistmanteli* - Cuticle-free coalified layer
- K *Kurtziana* sp. - Compression
- K *Kurtziana* sp. - Cuticle
- H *H. elongatum* - Compression
- L *L. tenison-woodsii* - Compression
- Y *L. steinmannii* - Compression
- S Indeterminate axis - Compression
- • Coal

Fig. 11. Principal component analysis[A]: plot of component scores. See text for explanation of PCA[A].

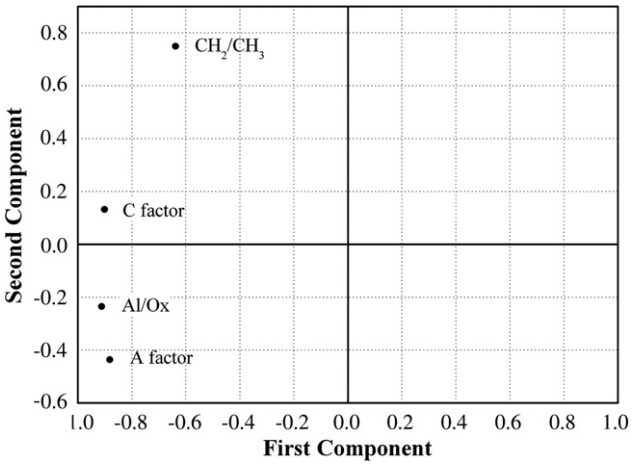

Fig. 13. Principal component analysis[B]: plot of component loadings.

discrimination between fossil taxa on the basis of functional groups (see the chemotaxonomic approach by D'Angelo et al., 2010). Some cuticle-sample groupings (see ellipses around *D. odontopteroides* and *J. coriacea* in Fig. 11) could be suggestive of the likely application of FTIR and subsequent PCA to chemotaxonomy. However, a larger data set, including an increased number of samples for each taxon, is desirable before obtaining more definite conclusions.

6.3.2. PCA[B] of the coaly forms: compressions, cuticle-free coalified layers and coals

A two-component solution (91.3% of the explained variance) is acceptable, despite the sharp drop in eigenvalue from 2.83 to 0.83, which we accept as explained. Figs. 13 and 14 show the loading plot and the component scores, respectively. A simplified plot (Fig. 15) exhibits the groupings of the different sample forms as indicated by delimiting ellipses around the groups, which are for clarity only.

The first component (70.7%) is negative with high loadings on Al/Ox and 'C' factor. This component is related to the presence of aliphatic and oxygen-containing functional groups. Compressions samples separate well from the other coaly forms (i.e., cuticle-free coalified layers and coal samples) and exhibit the most negative scores (Fig. 14, x axis). This is particularly evident in some specimens of *L. tenison-woodsii*, *D. odontopteroides* and *H. elongatum*, reflecting their comparatively higher contents of aliphatic and oxygen-containing groups (e.g., carbonyls). At the other extreme, some compressions (e.g., *L. steinmannii*, *D. odontopteroides* and the indeterminate axis) show low negative or even positive scores (Fig. 14, x axis).

The second component (20.6%) shows a high positive loading on CH_2/CH_3 and a moderate negative loading on 'A' factor (Fig. 13), likely reflecting the characteristics (length and degree of branching) of the polymethylenic chains vs. the changes in the relative intensity of aliphatic groups (Ganz and Kalkreuth, 1987).

Cuticle-free coalified layers exhibit the most positive scores (Fig. 14, y axis), indicating longer and less branched hydrocarbon side chains.

Coal samples separate well from cuticle-free coalified layers and exhibit negative scores against this component (Figs. 14 and 15, y axis) as a result of their shorter and more branched polymethylenic side chains (lower CH_2/CH_3 values in Table 4). Coal-sample grouping indicates clear differences regarding their functional groups, which are particularly evident in the lower contents of aliphatic and oxygen-containing groups, probably related to incrementally increased maturity.

Kerogen-type diagrams using only two IR variables (Figs. 8 and 9) indicate that compressions, cuticle-free coalified layers, and coals

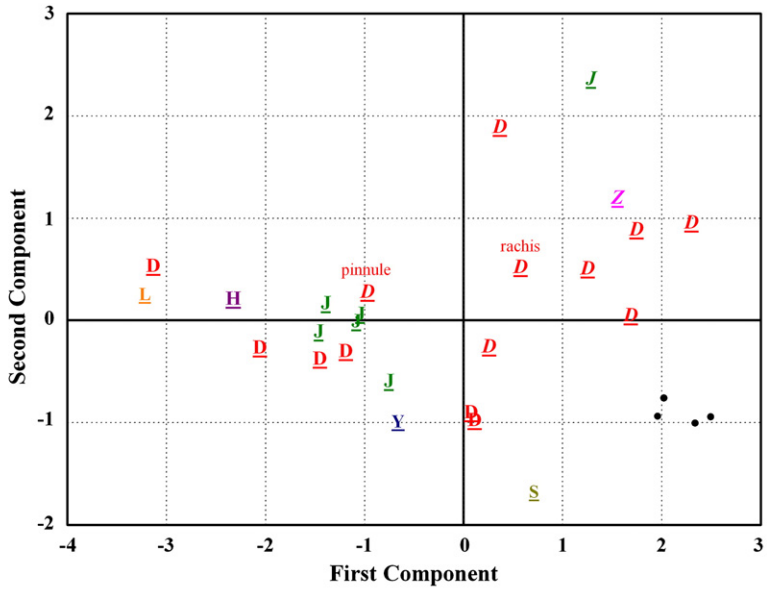

Legend

D *D. odontopteroides* - Compression
D *D. odontopteroides* - Cuticle-free coalified layer
J *J. coriacea* - Compression
J *J. coriacea* - Cuticle-free coalified layer
Z *Z. feistmanteli* - Cuticle-free coalified layer
H *H. elongatum* - Compression
L *L. tenison-woodsii* - Compression
Y *L. steinmannii* - Compression
S Indeterminate axis - Compression
• Coal

Fig. 14. Principal component analysis[B]: plot of component scores. See text for explanation of PCA[B].

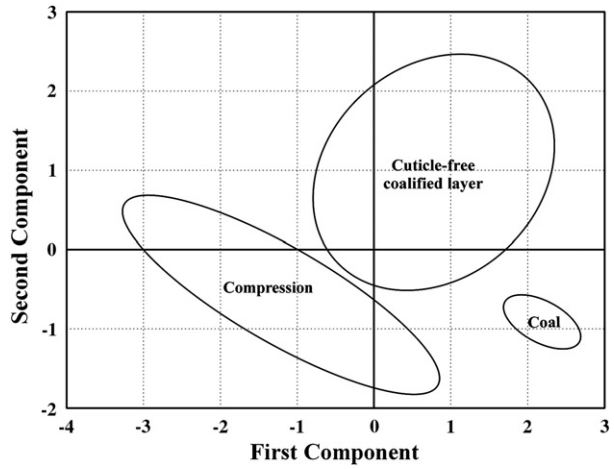

Fig. 15. Simplified plot of Fig. 14 indicating approximate regions of coaly sample forms (ellipses around the groups are for clarity only).

share similar functional groups. Furthermore, Figs. 11 and 12 (PCA[A]), emphasize the similarities among the three sample forms as revealed from the analysis of all the available FTIR variables. Finally, Figs. 14 and 15 (PCA[B]) leave little doubt about the usefulness of certain FTIR-derived variables (CH_2/CH_3, Al/Ox, 'A' factor and 'C' factor) for discriminating between coal samples and coaly fossil samples (i.e., compressions and cuticle-free coalified layers).

It is important to note that PCA[B] groupings coincide with an increasing maturity level of the different sample forms from compression to cuticle-free coalified layer to coal. The latter represents the more aromatic sample form with relatively lower contents of aliphatic and oxygen-containing compounds and shorter and more branched polymethylenic side chains.

7. Conclusions

This FTIR spectrometric study permits the following conclusions:

(i) The multivariate models support the distinction of different sample forms, i.e., (1) compressions, (2) cuticles, (3) cuticle-free coalified layers and (4) coals. The analysis of fossil remains sharing the same favorable thermal history, suggests a specimen-dependant diagenesis and the possibility of preservation of compounds (or molecular fragments) in the fossils, synthesized by the original organisms. In this respect, not ruled out is the likely chemotaxonomic utility of the FTIR technique to the study of co-occurring taxa (e.g., *Dicroidium* and *Johnstonia*).

(ii) Some common chemical characteristics exist between kerogen Types I, II and III and our data. This permits us to postulate that the functional groups characterizing the different sample forms could be related to the propensity to generate oil and gas/condensate from the kerogen.

(iii) Confirmed is the hypothesis of similarity between a compression fossil and its associated coal seam, provided thermo-integrity is maintained within the stratal section.

(iv) It is suggested that Schulze's process imitates some natural processes, which are involved in the formation of kerogen.

(v) The fossil material would lend itself to molecular taphonomy studies because of the favorable preservation states.

Acknowledgments

This work was supported by Universidad Nacional de Cuyo (SeCTyP Research Project 06/M012). M. E. Barbeito and J. Guzmán (Dirección de Estudios Tecnológicos e Investigaciones, Facultad de Ingeniería, Universidad Nacional de Cuyo) are gratefully acknowledged by the use of FTIR instruments. We thank Dr. Maria Mastalerz (Indiana Geological Survey, Indiana University, Bloomington) for the vitrinite reflection measurements of Cacheuta coal. A. Acosta, A. Menéndez and F. Marquat are thanked for assistance in the collection of samples.

Appendix A. Supplementary data

Supplementary data to this article can be found online at doi:10.1016/j.coal.2011.05.005.

References

Abu Hamad, A., Kerp, H., Vörding, B., Bandel, K., 2008. A Late Permian flora with *Dicroidium* from the Dead Sea region, Jordan. Review of Palaeobotany and Palynology 149, 85–130.

Anderson, T.W., 2003. An Introduction to Multivariate Statistical Analysis (Wiley Series in Probability and Statistics), Third ed. John Wiley & Sons, New Jersey. 752 pp.

Anderson, J.M., Anderson, H.M., 1983. Palaeoflora of Southern Africa. Molteno Formation (Triassic). Part 1 Introduction, Part 2 *Dicroidium*, vol. 1. Balkema, Rotterdam. 227 pp.

Anderson, H.M., Holmes, W.B.K., Fitness, L.A., 2008. Stems with attached *Dicroidium* leaves from the Ipswich Coal Measures, Queensland, Australia. Memoirs of the Queensland Museum 52, 1–12.

Archangelsky, S., 1968. Studies on Triassic fossil plants from Argentina. IV. The leaf genus *Dicroidium* and its possible relation to Rhexoxylon stems. Palaeontology 11, 500–512.

Artabe, A.E., 1990. Revalidación del género triásico *Zuberia* Frenguelli 1943, Familia Corystospermaceae. Revista del Museo de La Plata, nueva serie Paleontología 9, 145–157.

Artabe, A.E., Zamuner, A.B., Archangelsky, S., 1991. Estudios cuticulares en Cycadopsidas fósiles. El genero *Kurtziana* Frenguelli 1942. Ameghiniana 28, 365–374.

Baldoni, A.M., 1980. Revisión de las especies del género *Xylopteris* (Corystospermaceae) en el Triásico de Argentina, Australia y Sud África. Ameghiniana XVII, 135–155.

Bomfleur, B., Kerp, H., 2010. *Dicroidium* diversity in the Upper Triassic of north Victoria Land, East Antarctica. Review of Palaeobotany and Palynology 160, 67–101.

Bonetti, M.I.R., 1966. Consideraciones sobre algunos representantes de la Familia Corystospermaceae. Ameghiniana IV, 389–395.

Briggs, D.E.G., 1999. Molecular taphonomy of animal and plant cuticles: selective preservation and diagenesis. Philosophical Transactions of the Royal Society B: Biological Sciences 354, 7–17.

Collinson, M.E., van Bergen, P.F., Scott, A.C., de Leeuw, J.W., 1994. The oil-generating potential of plants from coal and coal-bearing strata through time: a review with new evidence from Carboniferous plants. In: Scott, A.C., Fleet, A.J. (Eds.), Coal and Coal-bearing Strata as Oil-prone Source Rocks? The Geological Society Publishing House, 77, Brassmill Lane, Bath, London, UK, pp. 31–70.

Collinson, M.E., Mösle, B., Finch, P., Scott, A.C., Wilson, R., 1998. Structure, biosynthesis and biodegradation of cutin and suberin. Ancient Biomolecules 2, 251–265.

Colthup, N.B., Daly, L.H., Wiberley, S.E., 1990. Introduction to Infrared and Raman Spectroscopy. Academic Press, New York. 547 pp.

D'Angelo, J.A., 2004. FT-IR determination of aliphatic and aromatic C–H contents of fossil leaf compressions. Part 2: applications. Anuario Latinoamericano de Educación Química 18, 34–38.

D'Angelo, J.A., 2006. Analysis by Fourier transform infrared spectroscopy of *Johnstonia* (Corystospermales, Corystospermaceae) cuticles and compressions from the Triassic of Cacheuta, Mendoza, Argentina. Ameghiniana 43, 669–685.

D'Angelo, J.A., Volkheimer, W., 2007. Searching for chemotaxonomic signals by Fourier Transform Infrared Spectroscopy in cuticles and compressions of perilacustrine remains of Corystospermales (Upper Triassic of Cacheuta, Mendoza, Argentina). 4th International Limnogeology Congress, Barcelona, Spain, pp. 206–207. Abstract.

D'Angelo, J.A., Zodrow, E.L., Mastalerz, M., 2007. Compression or cuticle — what is the difference? The Society for Organic Petrology Newsletter 24, 8–9.

D'Angelo, J.A., Zodrow, E.L., Camargo, A., 2010. Chemometric study of functional groups in Pennsylvanian gymnosperm plant organs (Sydney Coalfield, Canada): implications for chemotaxonomy and assessment of kerogen formation. Organic Geochemistry 41, 1312–1325.

D'Angelo, J.A., Volkheimer, W., Zodrow, E.L., in preparation. Cacheuta and Indiana paper coals: naturally macerated cuticles from FTIR viewpoint.

Durig, D.T., Esterle, J.S., Dickson, T.J., Durig, J.R., 1988. An investigation of the chemical variability of woody peat by FT-IR Spectroscopy. Applied Spectroscopy 42, 1239–1244.

Escudero, L.B., Volkheimer, W., D'Angelo, J.A., 2008. Variables derived from Fourier transform infrared cuticular spectra of *Dicroidium* and *Johnstonia*: a new proxy for paleo-CO_2 levels? XVII Congreso Geológico Argentino, Jujuy, Argentina. Abstract: 1005.

Frenguelli, J., 1941. *Sagenopteris* y *Linguifolium* del Lias de Piedra Pintada en el Neuquén (Patagonia). Notas del Museo de La Plata, 6. Paleontología 34, 405–437.

Frenguelli, J., 1948. Estratigrafía y edad del llamado "Rético" en la Argentina. Anales de la Sociedad Argentina de Estudios Geográficos. GAEA 8, 159–309.

Gallego, O.F., 1992. Conchostracos triásicos de Mendoza y San Juan. Ameghiniana 29, 159–175.
Ganz, H., Kalkreuth, W., 1987. Application of infrared spectroscopy to the classification of kerogen-types and the evolution of source rock and oil–shale potentials. Fuel 66, 708–711.
Gauglitz, G., Vo-Dinh, T., 2003. Handbook of Spectroscopy. WILEY-VCH Verlag GmbH & Co. KGaA, Weinheim. 538 pp.
Gnaedinger, S., Herbst, R., 2001. Pteridospermas triásicas del Norte Chico de Chile. Ameghiniana 38, 281–298.
Gothan, W., 1912. Über die Gattung *Thinnfeldia* Ettinghausen. Abhandlung Naturhistry Gesellrchoft Nürnberg 19, 67–80.
Guo, Y., Bustin, R.M., 1998. Micro-FTIR spectroscopy of liptinite macerals in coal. International Journal of Coal Geology 36, 259–275.
Gupta, N.S., Briggs, D.E.G., Collinson, M.E., Evershed, R.P., Michels, R., Jack, K.S., Pancost, R.D., 2007. Evidence for the *in situ* polymerisation of labile aliphatic organic compounds during preservation of fossil leaves: implications for organic matter preservation. Organic Geochemistry 38, 499–522.
Holmes, W.K.B., Anderson, H.M., 2005. The Middle Triassic megafossil flora of the Basin Creek Formation, Nymboida Coal Measures, New South Wales, Australia. Part 4. Ukomasiaceae. *Dicroidium* and affiliated fructifications. Proceedings of the Linnean Society of New South Wales 126, 1–37.
Ingle, J.D., Crouch, S.R., 1988. Spectrochemical Analysis. Prentice-Hall, New Yersey. 450 pp.
Izenman, A.J., 2008. Modern multivariate statistical techniques: regression, classification, and manifold learning (Springer texts in statistics), first ed. Springer, New York. 734 pp.
Jain, R., Delevoryas, T., 1967. A Middle Triassic Flora from the Cacheuta Formation, Minas de Petróleo, Argentina. Palaeontology 10, 564–589.
Jenchen, U., Rosenfeld, U., 2002. Continental Triassic in Argentina: response to tectonic activity. Journal of South American Earth Sciences 15, 461–479.
Johnson, R.A., Wichern, D.W., 2007. Applied Multivariate Statistical Analysis, sixth ed. Prentice Hall, New Jersey. 800 pp.
Jolliffe, I.T., 2002. Principal Component Analysis, second ed. Springer, New York. 487 pp.
Kaiser, H.F., 1960. The application of electronic computers to factor analysis. Educational and Psychological Measurement 20, 141–151.
Kendall, M.G., 1965. A Course in Multivariate Analysis. Third Impression. Charles Griffin & C. Ltd, London. 185 pp.
Kurtz, F., 1921. Atlas de plantas fósiles de la República Argentina. Actas de la Academia Nacional de Ciencias (Córdoba) 7, 129–153.
Largeau, C., Derenne, S., Casadevall, E., Berkaloff, C., Corolleur, M., Lugardon, B., Raynaud, J.F., Connan, J., 1990. Occurrence and origin of 'ultralaminar' structures in 'amorphous' kerogens of various source rocks and oil shales. Organic Geochemistry 16, 889–895.
Lattin, J., Carroll, D., Green, P., 2002. Analyzing Multivariate Data (Duxbury Applied Series), first ed. Duxbury Press, California. 560 pp.
Lin, R., Ritz, G.P., 1993a. Reflectance FT-IR microspectroscopy of fossil algae contained in organic-rich shale. Applied Spectroscopy 47, 265–271.
Lin, R., Ritz, G.P., 1993b. Studying individual macerals using i.r. Microspectroscopy, and implications on oil versus gas/condensate proneness and "low-rank" generation. Organic Geochemistry 20, 695–706.
Lis, G.P., Mastalerz, M., Schimmelmann, A., Lewan, M., Stankiewicz, B.A., 2005. FTIR absorption indices for thermal maturity in comparison with vitrinite reflectance Ro in type-II kerogen from Devonian black shales. Organic Geochemistry 36, 1533–1552.
Logan, G.A., Boon, J.J., Eglinton, G., 1993. Structural biopolymer preservation in Miocene leaf fossils from the Clarkia site, Northern Idaho. Proceedings of the National Academy of Sciences USA 90, 2246–2250.
López Gamundí, O.R., Espejo, I., Conaghan, P., Powell, C., 1994. Southern South America. In: Veevers, J.J., Powell, C. (Eds.), Permian-Triassic Pangean Basins and Foldbelts along the Panthalassan Margin of Gondwanaland: Geological Society of America, Memoir, 184, pp. 281–329.
Lyons, P.C., Orem, W.H., Mastalerz, M., Zodrow, E.L., Vieth-Redemann, A., Bustin, R.M., 1995. 13 C NMR, micro-FTIR and fluorescence spectra, and pyrolysis-gas chromatograms of coalified foliage of late Carboniferous medullosan seed ferns, Nova Scotia, Canada: implications for coalification and chemotaxonomy. International Journal of Coal Geology 27, 227–248.
Marsicano, C., Gallego, O.F., Arcucci, A., 2001. Faunas del Triásico: relaciones, patrones de distribución y sucesión temporal. In: Artabe, A.E., Morel, E., Zamuner, A.B. (Eds.), El Sistema Triásico en la Argentina. Fundación Museo de La Plata, La Plata, pp. 131–141.
Mastalerz, M., Bustin, R.M., 1993a. Variation in maceral chemistry within and between coals of varying rank: an electron microprobe and micro-FTIR investigation. Journal of Microscopy 171, 153–166.
Mastalerz, M., Bustin, R.M., 1993b. Electron microprobe and micro-FTIR analyses applied to maceral chemistry. International Journal of Coal Geology 24, 333–345.
Mastalerz, M., Bustin, R.M., 1996. Application of reflectance micro-Fourier Transform infrared analysis to the study of coal macerals: an example from the Late Jurassic to Early Cretaceous coals of the Mist Mountain Formation, British Columbia, Canada. International Journal of Coal Geology 32, 55–67.
Miltner, A., Zech, W., 1998. Beech leaf litter degradation and transformation as influenced by mineral phases. Organic Geochemistry 28, 457–463.
Morel, E.M., 1994. El Triásico del cerro Cacheuta, Mendoza (Argentina). Parte I. Geología, contenido florístico y cronoestratigrafía. Ameghiniana 31, 161–176.
Morel, E.M., Povilauskas, L., 2002. Addenda a la flora triásica de la Formación Potrerillos en el cerro Cacheuta, provincia de Mendoza, Argentina. Ameghiniana 39, 501–503.
Morel, E.M., Artabe, A.E., Spalletti, L.A., 2003. Triassic floras of Argentina: biostratigraphy, floristic events and comparison with other areas of Gondwana and Laurasia. Alcheringa 27, 231–243.
Morel, E.M., Artabe, A.E., Ganuza, D.G., Zúñiga, A., 2010. La paleoflora triásica del cerro Cacheuta, provincia de Mendoza, Argentina. Bryopsida, Lycopsida, Sphenopsida, Filicopsida y Gymnospermopsida (Corystospermales y Peltaspermales). Ameghiniana 47, 3–23.
Mösle, B., Collinson, M.E., Finch, P., Stankiewicz, A., Scott, A.C., Wilson, R., 1998. Factors influencing the preservation of plant cuticles: a comparison of morphology and chemical composition of extant and fossil examples. Organic Geochemistry 29, 1369–1380.
Niklas, K.J., Giannasi, D.E., 1978. Angiosperm paleobiochemistry of the Succor Creek flora (Miocene) Oregon, USA. American Journal of Botany 65, 943–952.
Nip, M., Tegelaar, E.W., Brinkhuis, H., de Leeuw, J.W., Schenck, P.A., Holloway, P.J., 1986a. Analysis of modern and fossil plant cuticles by Curie point Py-GC and Curie point Py-GC-MS: recognition of a new, highly aliphatic and resistant biopolymer. Organic Geochemistry 10, 769–778.
Nip, M., Tegelaar, E.W., de Leeuw, J.W., Schenck, P.A., 1986b. A new non-saponifiable highly aliphatic and resistant biopolymer in plant cuticles. Naturwissenschaften 73, 579–585.
Painter, P.C., Snyder, R.W., Starsinic, M., Coleman, M.M., Kuehn, D.W., Davis, A., 1981. Concerning the application of FT-IR to the study of coal: a critical assessment of band assignments and the application of spectral analysis programs. Applied Spectroscopy 35, 475–485.
Pattemore, G.A., Rigby, J.F., 2005. Fructifications and foliage from the Mesozoic of southeast Queensland. Memoirs of the Queensland Museum 50, 329–345.
Paull, R., Michaelsen, B.H., Mc Kirdy, D.M., 1998. Fernenes and other triterpenoid hydrocarbons in *Dicroidium*-bearing Triassic mudstone and coals from South Australia. Organic Geochemistry 29, 1331–1344.
Petriella, B., 1979. Sinopsis de las Corystospermaceae (Corystospermales, Pteridospermophyta) de Argentina. I. Hojas. Ameghiniana XVI, 81–102.
Petriella, B., 1981. Sistemática y vinculaciones de las Corystospermaceae H. Thomas. Ameghiniana XVIII, 221–234.
Petriella, B., 1985. Caracteres adaptativos y autoecología de las Corystospermaceae. In: Weber, R. (Ed.), III Congreso Latinoamericano de Paleontología (México). Simposio sobre floras del triásico tardío, su fitogeografía y paleogeografía. Memorias del Instituto Geológico de la Universidad Nacional Autónoma de México, México, pp. 53–57.
Pšenička, J., Zodrow, E.L., Mastalerz, M., Bek, J., 2005. Functional groups of fossil marattialeans: chemotaxonomic implications for Pennsylvanian tree ferns and pteridophylls. International Journal of Coal Geology 61, 259–280.
Rencher, A.C., 2002. Methods of multivariate analysis, second ed. Wiley Series in Probability and Statistics Series, vol. 1. John Wiley & Sons, New Jersey. 738 pp.
Retallack, G.J., 1977. Reconstructing Triassic vegetation of eastern Australasia: a new approach for the biostratigraphy of Gondwanaland. Alcheringa 1, 247–278.
Retallack, G.J., 1980. Middle Triassic megafossil plants and trace fossils from Tank Gully, Canterburry, New Zealand. Journal of the Royal Society of New Zealand 10, 31–63.
Retallack, G.J., 1981. Middle Triassic megafossil plants from Long Gully, near Otematata, north Otago, New Zealand. Journal of the Royal Society of New Zealand 11, 167–200.
Rolleri, E.O., Criado Roque, P., 1968. La cuenca triásica del norte de Mendoza. Jornadas Geológicas Argentinas (Comodoro Rivadavia, 1966): Actas, 1, pp. 1–76.
Shurvell, H.F., 2002. Spectra-structure correlations in the mid- and far-infrared. In: Chalmers, J., Griffiths, P. (Eds.), Handbook of Vibrational Spectroscopy. : Sample Characterization and Spectral Data Processing, 3. John Wiley & Sons Ltd, Chichester, pp. 1–611.
Sobkowiak, M., Painter, P., 1992. Determination of the aliphatic and aromatic CH contents of coals by FT-i.r.: studies of coal extracts. Fuel 71, 1105–1125.
StatSoft Inc, 2001. STATISTICA (Data Analysis Software System), Version 6. www.statsoft.com.
Stipanicic, P.N., 1979. El Triásico del valle del río de los Patos (Provincia de San Juan). Geología Regional Argentina, Segundo Simposio, 1976, Academia Nacional de Ciencias I, pp. 695–744.
Stipanicic, P.N., Zavattieri, A.M., 2002. Uspallata (Grupo). In: Stipanicic, P.N., Marsicano, C.A. (Eds.), Léxico Estratigráfico de la Argentina, Volumen VIII: Triásico. Asociación Geológica Argentina, 26, Buenos Aires, Argentina, pp. 290–294.
Stipanicic, P.N., Herbst, R., Bonetti, M.I.R., 1995. Floras Triásicas. In: Stipanicic, P.N., Hünicken, M.A. (Eds.), Contribuciones a la Palaeophytologia Argentina. Revisión y Actualización de la Obra Paleobotánica de Kurtz en la República Argentina, Actas de la Academia Nacional de Ciencias, XI, Córdoba, pp. 127–184.
Stuart, B., 2004. Infrared Spectroscopy: Fundamentals and Applications. John Wiley & Sons Ltd., England. 224 pp.
Taylor, T.N., Taylor, E.L., Krings, M., 2009. The Biology and Evolution of Fossil Plants, second ed. Academic Press, New York. 1230 pp.
Tegelaar, E.W., Kerp, H., Visscher, H., Schenck, P.A., de Leeuw, J.W., 1991. Bias of the palaeobotanical record as a consequence of variations in the chemical composition of higher vascular plant cuticles. Palaeobiology 17, 133–144.
Townrow, J.A., 1957. On *Dicroidium*, probably a pteridospermous leaf and other leaves now removed from this genus. Transactions of the Geological Society of South Africa 60, 21–56.
van Bergen, P.F., Blokker, P., Collinson, M.E., Sinninghe Damsté, J.S., de Leeuw, J.W., 2004. Structural miomocromolecules in plants: what can be learnt from the fossil record? In: Hemsley, A.R., Poole, A.I. (Eds.), The Evolution of Plant Physiology. Elsevier Acad Press, Oxford, pp. 133–154.
Walkom, A.B., 1925. Notes on some Tasmanian Mesozoic plants. Part 1. Papers and Proceedings of the Royal Society of Tasmania (1924), pp. 73–89.

Wang, S.H., Griffiths, P.R., 1985. Resolution enhancement of diffuse reflectance i.r. spectra of coals by Fourier self-deconvolution. 1. C–H stretching and bending modes. Fuel 64, 229–236.

Zamuner, A.B., Zavattieri, A.M., Artabe, A.E., Morel, E.M., 2001. Paleobotánica. In: Artabe, A.E., Morel, E., Zamuner, A.B. (Eds.), El Sistema Triásico en la Argentina. Fundación Museo de La Plata, La Plata, pp. 143–184.

Zodrow, E.L., Cleal, C.J., 1998. Revision of the pteridosperm foliage *Alethopteris* and *Lonchopteridium* (Upper Carboniferous), Sydney Coalfield, Nova Scotia, Canada. Palaeontographica Abteilung B. 247, 65–122.

Zodrow, E.L., Mastalerz, M., 2001. Chemotaxonomy for naturally macerated tree-fern cuticles (Medullosales and Marattiales), Carboniferous Sydney and Mabou Sub-Basins, Nova Scotia, Canada. International Journal of Coal Geology 47, 255–275.

Zodrow, E.L., Mastalerz, M., 2002. FTIR and py-GC-MS spectra of true-fern and seed-fern sphenopterids (Sydney Coalfield, Nova Scotia, Canada, Pennsylvanian). International Journal of Coal Geology 51, 111–127.

Zodrow, E.L., Mastalerz, M., 2007. Functional groups in a single pteridosperm species: variability and circumscription (Pennsylvanian, Nova Scotia, Canada). International Journal of Coal Geology 70, 313–324.

Zodrow, E.L., Mastalerz, M., 2009. A proposed origin for fossilized Pennsylvanian plant cuticles by pyrite oxidation (Sydney Coalfield, Nova Scotia, Canada). Bulletin of Geosciences 84, 227–240.

Zodrow, E.L., Mastalerz, M., Orem, W.H., Šimůnek, Z., Bashforth, A.R., 2000. Functional groups and elemental analyses of cuticular morphotypes of *Cordaites principalis* (Germar) Geinitz, Carboniferous Maritimes Basin, Canada. International Journal of Coal Geology 45, 1–19.

Zodrow, E.L., Mastalerz, M., Šimůnek, Z., 2003. FTIR-derived characteristics of fossil-gymnosperm leaf remains of *Cordaites principalis* and *Cordaites borassifolius* (Pennsylvanian, Maritimes Canada and Czech Republic). International Journal of Coal Geology 55, 95–102.

Zodrow, E.L., D'Angelo, J.A., Mastalerz, M., Keefe, D., 2009. Compression-cuticle relationship of seed ferns: Insights from liquid–solid FTIR (Late Palaeozoic–Early Mesozoic, Canada–Spain–Argentina). International Journal of Coal Geology 79, 61–73.

Zodrow, E.L., D'Angelo, J.A., Mastalerz, M., Cleal, C., Keefe, D., 2010. Phytochemistry of the fossilized-cuticle frond *Macroneuropteris macrophylla* (Pennsylvanian seed fern, Canada). International Journal of Coal Geology 84, 71–82.

Zuber, R., 1887. Estudio geológico del Cerro Cacheuta y sus contornos (República Argentina–Provincia de Mendoza). Boletín de la Academia Nacional de Ciencias (Córdoba) 10, 448–472.